The Korean Journal of Ceramics, **5** [1] 1 - 11 (1999)

Space Charge Effect on Grain Growth Kinetics of Tetragonal Zirconia Polycrystal

Uong Chon

Research Institute of Industrial Science and Technology (RIST), Pohang City, Kyungbuk 790-330, Korea
(Received October 16, 1998)

The effect of aliovalent dopants, Nb_2O_5 and MnO, on the grain growth kinetics of 12 mol% ceria stabilized tetragonal zirconia polycrystals (Ce-TZP) was studied. All specimens were sintered at 1550°C for 20 minutes prior to annealing at different temperatures to study grain growth kinetics. Grain growth kinetics of Ce-TZP and 1 mol% Nb_2O_5 doped Ce-TZP (Ce-TZP/Nb_2O_5) during annealing at 1475, 1550, and 1600°C adequately matched with square law ($D^2-D_o^2=k_st$). However, grain growth in 1 mol% MnO doped Ce-TZP (Ce-TZP/MnO) annealed at 1550°C obeyed the cubic law of grain-growth. While MnO suppressed grain growth in Ce-TZP by drag force exerted by Mn^{+2} ions which segregated strongly to the positively-charged grain boundaries of Ce-TZP, Nb_2O_5 enhanced grain growth by increasing the concentrations of vacancies of Zr^{+4} ion and Ce^{+4} ions. Surface analysis with X-ray photoelectron spectroscopy (XPS) showed the segregation of Mn^{+2} ions to grain boundaries. The kinetics of grain growth obtained in the base Ce-TZP and the Ce-TZPs with the aliovalent dopants were examined in the context of impurity drag effect and space charge effect.

Key words : TZP, Aliovalent dopant, Grain growth kinetics, Space charge effect

I. Introduction

The investgation of zirconia ceramics has continued to attract the interest of ever increasing numbers of scientists and technologists as many potential commercial applications for these engineering ceramics have been identified.[1,2] The traditional properties associated with ceramics, i. e. brittleness and weakness, have been improved with high fracture toughness and high strength by the advent of zirconia ceramics. Pure zirconia exhibits three types of polymorphs.[1,3] The monoclinic phase is stable up to about 1170°C. At this temperature it transforms to the tetragonal phase which in turn is stable up to 2370°C where the cubic phase forms and is stable up to the melting point of 2680°C. The properties of zirconia can be modified significantly by the addition of one of the oxides, CaO, MgO, Y_2O_3, or CeO_2.[4-7] Addition of appropriate amounts of one of these oxides stabilizes the tetragonal phase at room temperature.[8-13] 12 mol % ceria-stabilized zirconia (Ce-TZP) at room temperature typically consists of nearly 100 percent of the tetragonal grains. The tetragonal to monoclinic transformation occurs on supercooling below room temperature[1-3] because the tetragonal phase is metastable at room temperature. The tetragonal to monoclinic transformation is martensitic with an accompanying volume-increase. The transformation temperature is dependent on the grain size,[14-15] grain shape,[17-18] composition,[19] applied stress[16] and etc.

There are optimum amount of stabilizer and grain size for maximizing strength and fracture toughness of zirconia ceramics. In the case of zirconia ceramics stabilized with CeO_2, Ce-TZP ceramics show maximum fracture toughness at about 12 mol % CeO_2.[20]

Grain size can affect various properties of ceramics. In partially-stabilized zirconias including PSZs and TZPs, the stress-induced martensitic transformation of the metastable tetragonal phase to the monoclinic phase, which is responsible for the enhanced fracture toughness via transformation toughening, is strongly affected by the grain size. This grain-size dependence is reflected in a variation of the transformation yield stress with grain size as well as the observation of a critical grain size above which the tetragonal phase can not be retained at room temperature. Therefore, the phase stability of tetragonal zirconia particles embedded in the matrix of Ce-TZP, which is very important to the mechanical properties of zirconia ceramics, depends strongly on grain size and impurities.[14,21]

The grain growth of ceramic materials is affected by impurities, porosity, and second-phase particles. In Ce-TZP in which Ce forms a single-phase solid solution with zirconia with near theoretical density after sintering, the solid-solution impurity is the most important factor affecting grain growth.[22-24] In pure polycrystalline ceramic materials, grain boundaries are normally charged with an associated space charge cloud in which the concentration of lattice defects is different from the concentration far from grain boundary. If a polycrystalline ceramics contain small amounts of impurities, the segregations of impurities at grain boundaries and the degrees by which the free energy is lowered is directly related to the

amount of impurities segregated to the grain boundaries. The amount of impurities segregated on grain boundary mainly depends on the Coulombic force between impurities with effective charges and charged grain boundaries caused by ionic property of the ceramic materials.[25-26] The addition of aliovalent dopants affects the grain growth kinetics in two ways, (1) enhancement or reduction of solute concentrations near the grain boundary and (2) enhancement or reduction of lattice defect concentrations near the grain boundary.[26] If solutes segregate to the grain boundary, the grain boundary energy and the grain boundary velocity decrease due to the drag exerted by the slowly diffusing solutes as the amount of solutes segregated on grain boundary increases.[27-30] If the enhancement of lattice defect concentration near grain boundary is considered, the grain boundary velocity increases significantly due to the enhancement of diffusivity of lattice ions.[31-33]

The amount of solute segregation is determined primarily by electrostatic potential formed between grain boundary and the solute atoms. Also the size of the solute ions also affects the behavior of the solute segregation.[22] Therefore we can control the grain growth of ceramic materials by the addition of small amount of dopants.

II. Experimental Procedure

88 mol% of zirconia powder and 12 mol% of ceria powder were weighed and put in a polyethylene bottle with adequate zirconia milling media and ethyl alcohol, and milled for 24 hours. The milled slurry was dried in air. The dried powder was calcined in air at 950°C for 1 hour. Doping was achieved by adding 1 mol% of dopant oxides to the calcined powder of the base Ce-TZP, and then ball milling in ethanol for 24 hours, and drying in air. The dried powder mixture was screened through a 75 μm screen. The screened powder was pressed uniaxially in a die press at 35 MPa, followed by isostatic pressing at 207 MPa. The green compacts were sintered at 1550°C for 20 minutes and then annealed at 1475, 1550, and 1600°C for different time intervals. Bulk densities were measured after sintering using Archimedes method with distilled water as the immersion medium.

1. Grain size measurement

For the study of grain growth kinetics the as-annealed specimens were cut, ground, and polished. Polishing with 15, 6 and 1 μm diamond paste was executed for surface finish. To reveal the microstructure, the polished specimens were thermally etched at 1400°C for 40 minutes and coated with gold by sputter coater for examination by scanning electron microscope (SEM). The average grain size, D, was determined by measuring the average grain intercept length, L, on scanning electron micrographs of polished and thermally-etched surface of each of the specimens, where D and L are related by equation 1.

$$D=1.57\ L \quad (1)$$

A digital planometer# was used to evaluate the intercept lengths of over 700 grains in each specimen.

2. Chemical analysis of the grain boundary and grain bulk phase

Examination of fracture surfaces of all the Ce-TZPs with SEM showed intergranular fracture modes at room temperature. Thus, all fracture surfaces represented grain boundary areas. Grain bulk phase could be examined on transgranular surface polished to 1 μm, although the polished surface included a negligible amount of grain boundaries. Since the signals of X-ray photoelectron spectroscopy (XPS) and Auger electron spectroscopy (AES) come primarily from elements within a distance of 1 to 2 nm from the surface, these techniques were used to analyze the compositions of grain boundary and grain bulk. The intensities of peaks were obtained by measuring the areas below the peaks in XPS and the heights of peaks in AES. The concentrations of solutes at grain boundaries and grain bulks were measured by determining the amount of solute cations relative to that of the zirconium ions. The sensitivity factors were taken from reference 34. Since AES examines a local area of specimen while XPS examines the whole surface area, XPS measurements were used to assess relative segregation of the cation dopants.

III. Results

1. Grain growth in the base Ce-TZP

The as-sintered specimens of Ce-TZP had approxima-

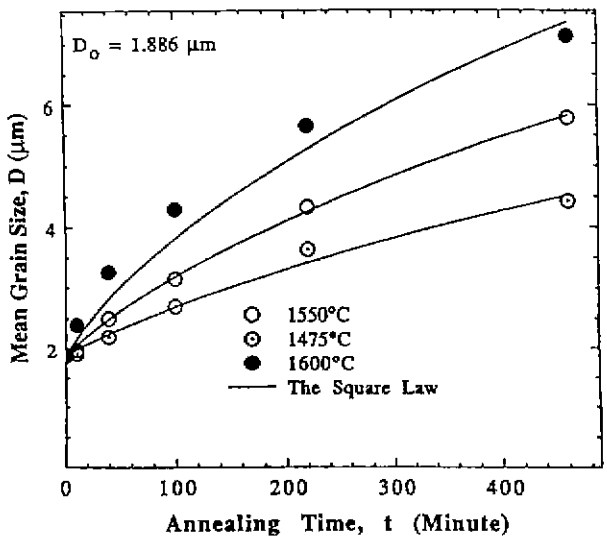

Fig. 1. The growth of mean grain size, D, of Ce-TZP sintered at 1550°C for 20 minutes and annealed at different temperatures and different times with the square law of grain-growth.

#Numonic Digitizer 1224, Numonics Co., Lansdale, PA

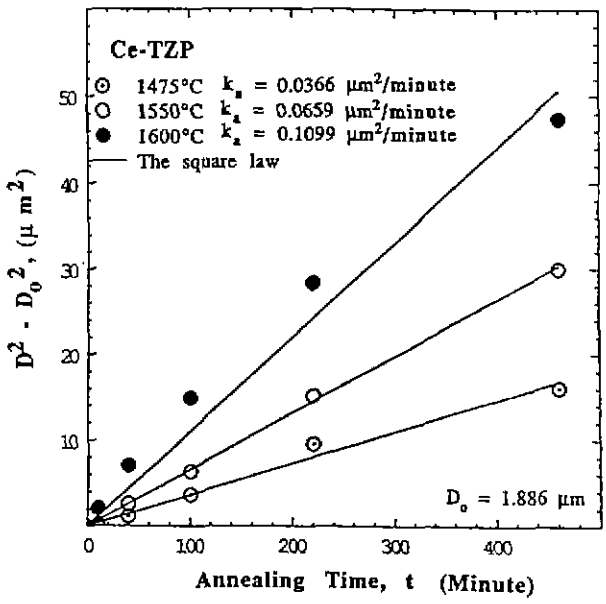

Fig. 2. The variation of the k_a values with the annealing temperature.

tely 97% of theoretical density and after annealing the density increased to 99% of it. The variations of the average grain size in the base Ce-TZP with the annealing time at the three temperatures are shown with the square law of grain-growth ($D^2-D_o^2=k_at$) in Fig. 1. To assess the grain-growth constants, k_a, at the three temperatures, $D^2-D_o^2$ was plotted versus t as shown in Fig. 2. The good linearity obtained in Fig. 2 further supported the use of square grain-growth law to describe grain-growth kinetics in the base Ce-TZP. The value of k_a increased as the annealing temperature increased. The temperature dependence of the grain-growth constant for the base Ce-TZP is shown in the Arrhenius plot of Fig. 3.

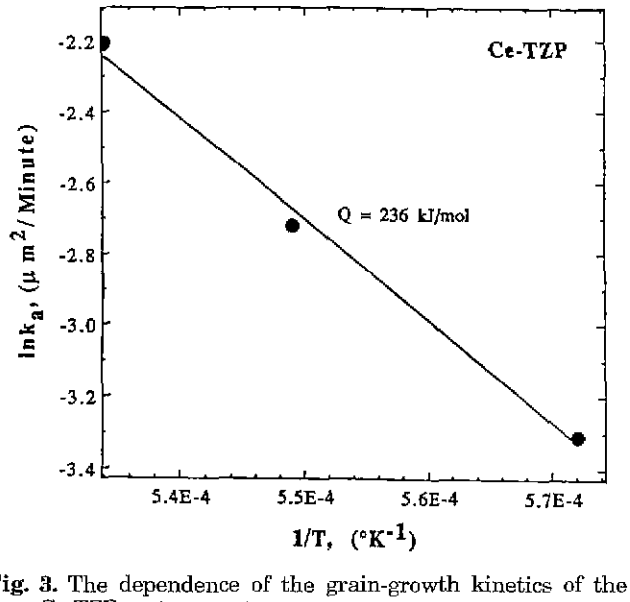

Fig. 3. The dependence of the grain-growth kinetics of the base Ce-TZP on temperature.

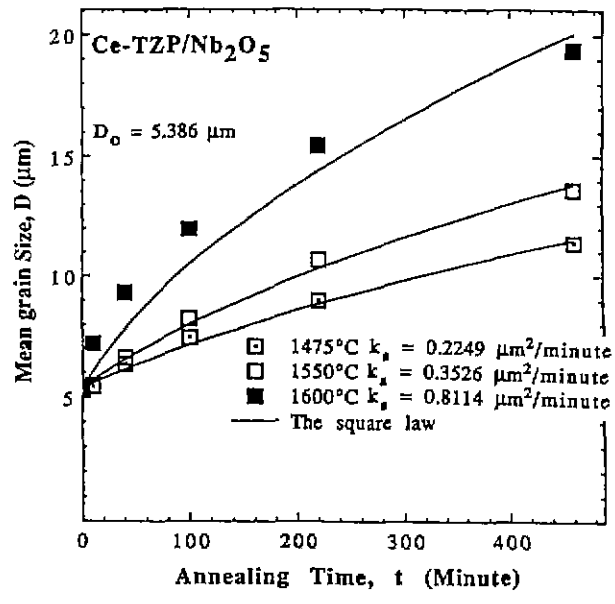

Fig. 4. The growth of mean grain size, D, of Ce-TZP/Nb_2O_5 sintered at 1550°C for 20 minutes and annealed at different temperatures and different times with the square law of grain-growth.

The linear plot of Fig. 3 suggested the following temperature dependence for ka.

$$k_a(T)=k_{ao}\exp(-Q/RT) \quad (2)$$

Analysis of the data of Fig. 3 in terms of Equation 2 gave $k_{ao}=4.166\times10^5$ μm²/minute and Q=236 kJ/mole.

2. Effects of Nb_2O_5 and MnO on grain growth kinetics of the base Ce-TZP

Fig. 4 shows the variation of the average grain size with annealing time at the three temperatures for Ce-TZP/Nb_2O_5 with square law. As it was the case in the base Ce-TZP, it was found that the grain-growth kinetics of Ce-TZP/Nb_2O_5 annealed at 1475, 1550°C and 1600°C matched with the square law. The grain-growth constant, k_a, increased as the annealing temperature increased and the value of k_a for Ce-TZP/Nb_2O_5 at each temperature was much higher than the corresponding values of k_a for the base Ce-TZP. Thus, Nb_2O_5 enhanced the grain-growth kinetics of Ce-TZP. From the Arrehnius plot to determined the activation energy for the grain growth in Ce-TZP/Nb_2O_5 in Fig. 5 the value of k_{ao} and Q was found to be 2.117×10^7 μm²/minute and 268 kJ/mole respectively. The activation energy for grain growth in Ce-TZP/Nb_2O_5 was, thus, approximately the same as that for the base Ce-TZP. Grain growth in Ce-TZP/MnO annealed at 1550°C also followed the cubic law, as shown in Fig. 6 and the grain-growth constant, k_a, was 0.0821 μm³/minute. The grain-growth constant, k_a, decreased relative to that of the base Ce-TZP at the same annealing temperature. From a comparison of the microstructures and grain-growth kinetics in the base Ce-TZP and the doped Ce-TZPs the following

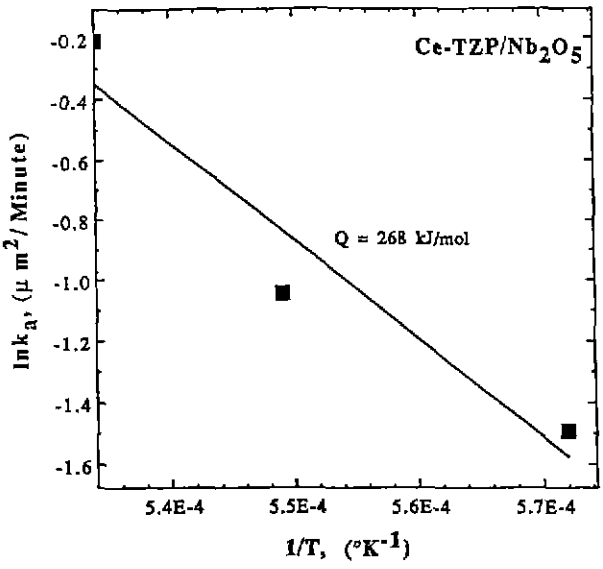

Fig. 5. The dependence of the grain-growth kinetics of the Ce-TZP/Nb_2O_5 on temperature.

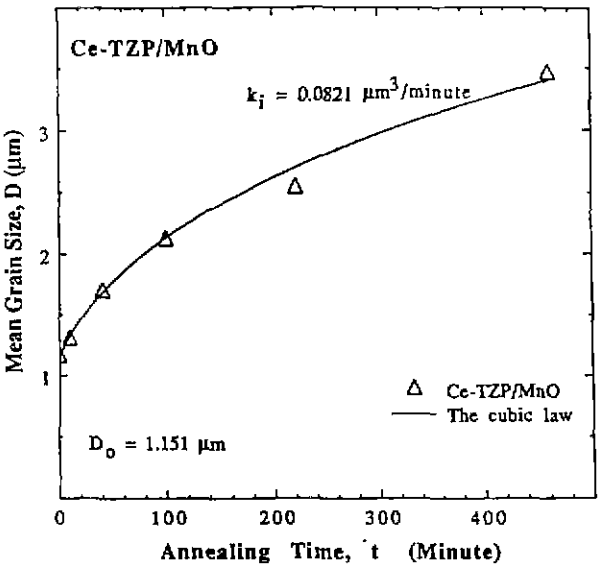

Fig. 6. The growth of mean grain size, D, of Ce-TZP/MnO sintered at 1550°C for 20 minutes and annealed at 1550°C *and for different times with the cubic law of grain-growth.*

observations were made: 1) MnO suppressed grain growth while Nb_2O_5 significantly enhanced grain growth of the tetragonal zirconia phase in the Ce-TZP. 2) MnO promoted more uniform grain size.

3. Surface Analysis of the Base and Doped Ce-TZPs

The base and doped Ce-TZPs sintered at 1550°C for 20 minutes was used for the surface analysis. The entire examination of spectra of AES and XPS taken from the intergranularly fractured surfaces and the polished surfaces of the both Ce-TZPs was executed. The intergranularly fractured surface and the polished surface represent grain-boundary area and grain-bulk area, respectively.

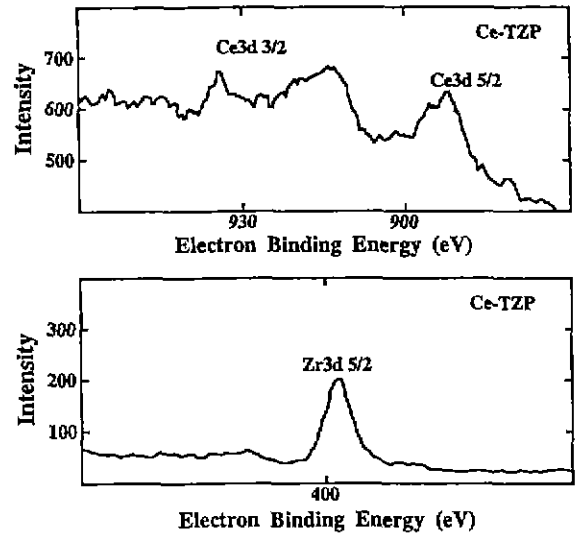

Fig. 7. The detailed XPS spectra of cerium ions and zirconium ion in the grain boundary of the base Ce-TZP sintered at 1550°C for 20 minutes.

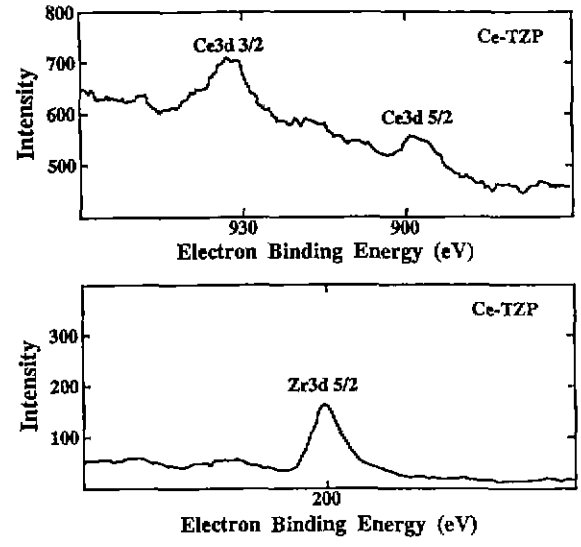

Fig. 8. The detailed XPS spectra of cerium ions and zirconium ion in the grain bulk of the base Ce-TZP sintered at 1550°C for 20 minutes.

Detailed spectra of XPS of cerium ions (Ce^{+3} and Ce^{+4} ions) and zirconium ion (Zr^{+4} ion) on grain boundaries and grain bulk in the base Ce-TZP, respectively in Fig. 7 and 8. From the starting composition of the base Ce-TZP (12 mol % CeO_2 and 88 mol % ZrO_2) one would expect that the molar concentration of cerium ions relative to that of the host zirconium ion should be 0.136. From quantitative analysis it was found that the concentrations of the cerium ions relative to that of the zirconium ion in the grain-boundary area and grain-bulk area were 0.175 and 0.138, respectively. Thus, the concentration of the cerium ions measured in the grain bulk agreed with the starting composition of the base Ce-TZP. From the XPS spectra of Ce-TZP/Nb_2O_5 in Fig. 9 and 10 the relative con-

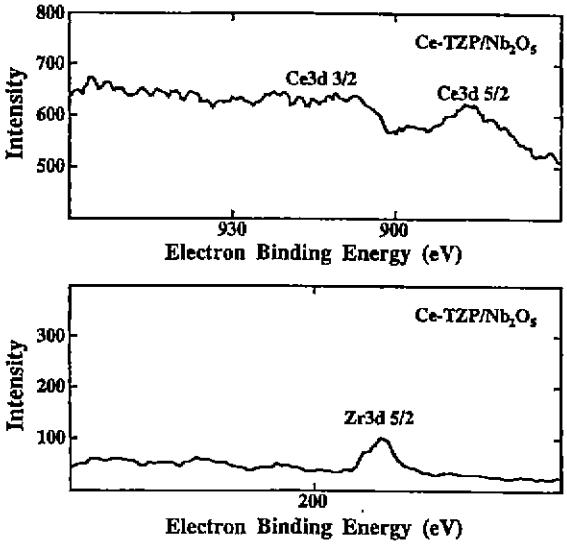

Fig. 9. The detailed XPS spectra of cerium ions and zirconium ion in the grain boundary of the Ce-TZP/Nb_2O_5 sintered at 1550°C for 20 minutes.

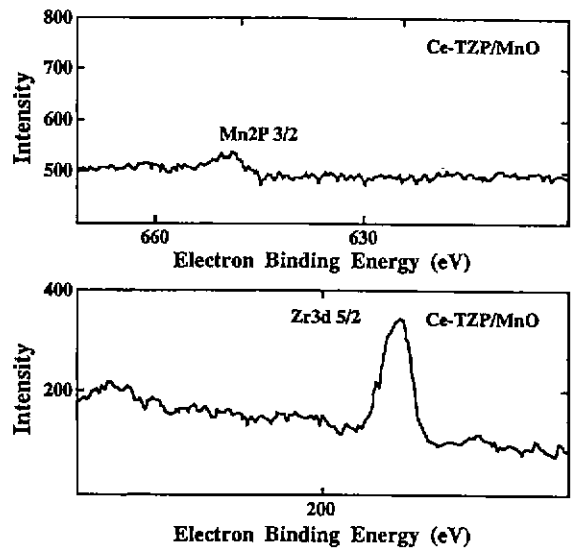

Fig. 11. The detailed XPS spectra of manganese ion in the grain boundary of the Ce-TZP/MnO sintered at 1550°C for 20 minutes.

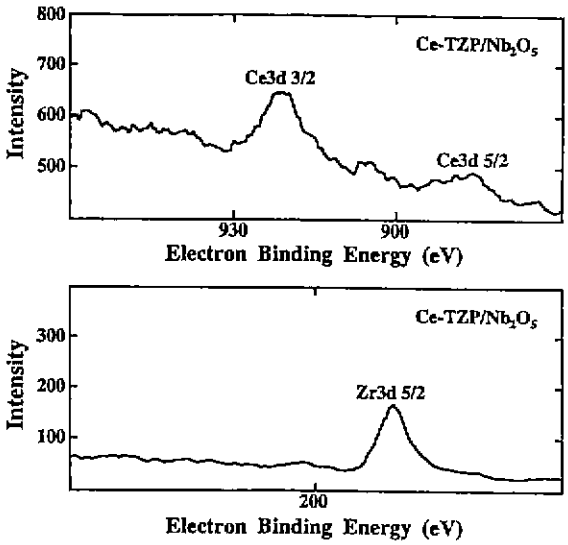

Fig. 10. The detailed XPS spectra of cerium ions and zirconium ion in the grain bulk of the Ce-TZP/Nb_2O_5 sintered at 1550°C for 20 minutes.

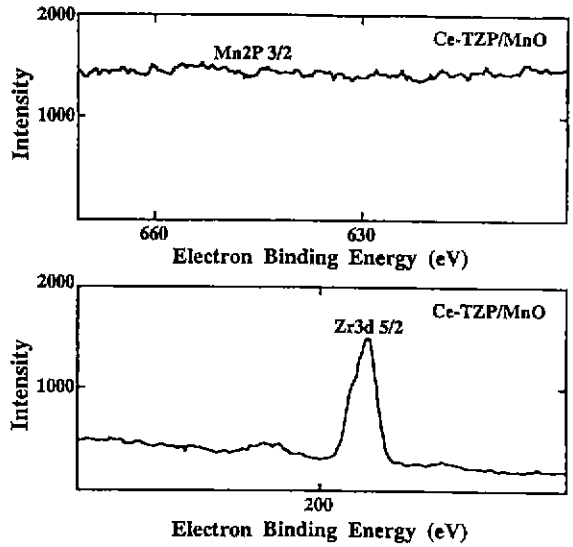

Fig. 12. The detailed XPS spectra of manganese ion in the grain bulk of the Ce-TZP/MnO sintered at 1550°C for 20 minutes.

centrations of cerium ion in the grain-boundary and bulk area were calculated and found to be 0.177 and 0.137, respectively. Although the XPS spectra did not show a peak corresponding to the niobium ions it is evident from the relative heights of the niobium and the zirconium ions in the AES spectra obtained from the grain-boundary and grain-bulk areas that the concentration of the niobium ions was greater in the grain-bulk than at the grain boundaries. This suggested that the niobium ions were repelled by the grain boundaries and they were predominantly located in the grain bulk. Peaks corresponding manganese ion was not found in the detailed spectrum of the grain bulk in Fig. 11 and 12 due to its low sensitivity factor as well as a low concentration of Mn^{+2} ion in the grain bulk. For quantitative analysis the concentration of Mn^{+2} ion in the grain bulk was assumed to be 1 mol %. From that assumption, the concentrations of Mn^{+2} ion relative to that of the host zirconium ion in the grain-boundary area and the grain bulk area were 0.077 and 0.012, respectively. The segregation factors of the cerium ions and the dopant ions from the detailed spectra of XPS were determined using the following equation

$$S_D=(P_{D(B)}/\xi_D)/(P_{Zr(B)}/\xi_{Zr})/(P_{D(o)}/\xi_D)/(P_{Zr(o)}/\xi_{Zr}) \quad (3)$$

Where S_D is the segregation factor for the cerium ions (or the dopant ion), $P_{D(B)}$ and $P_{Zr(B)}$ are the integrated inten-

Table 1. Segregation Factors of the Cerium Ions and the Dopant ion for Ce-TZP, Ce-TZP/Nb_2O_5 and Ce-TZP/MnO

Material	The segregation factor, S, of the cerium ions	The segregation factor, S, of the dopant ions
Ce-TZP	1.3	-
Ce-TZP/Nb_2O_5	1.3	-
Ce-TZP/MnO	-	6.4

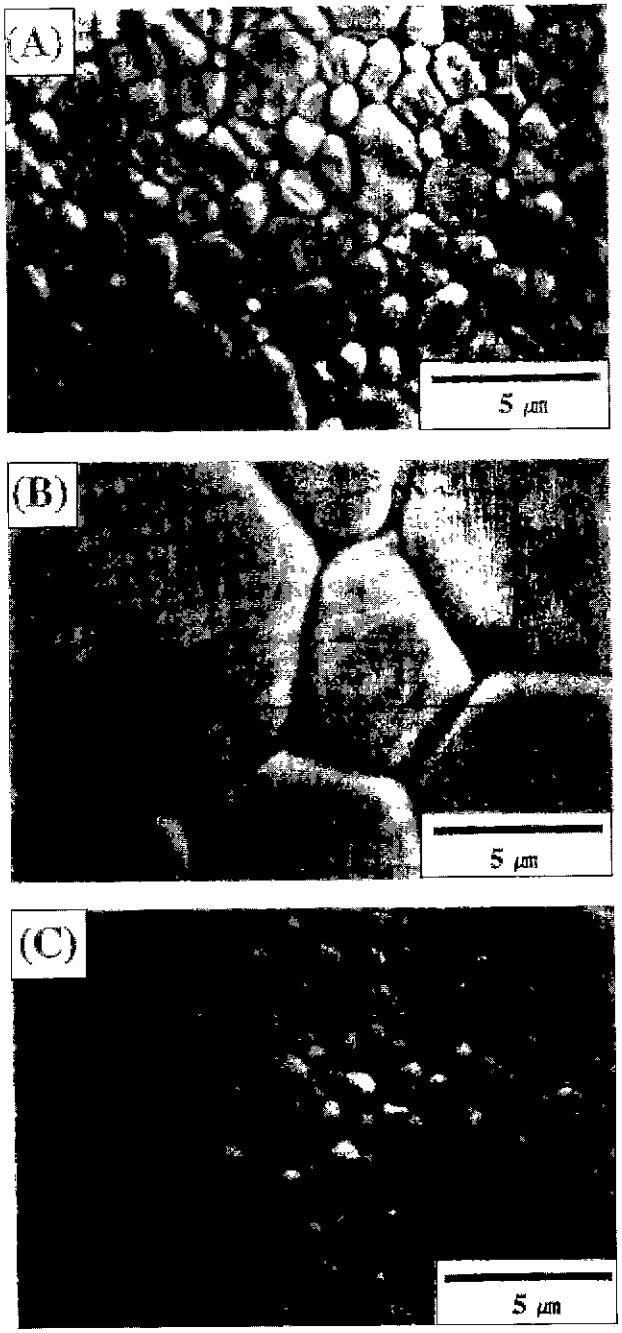

Fig. 13. The comparison of microstructures of (A) Ce-TZP, (B) Ce-TZP/Nb_2O_5 (C) Ce-TZP/MnO sintered at 1550°C for 20 minutes and annealed at 1550°C for 1 hour 40 minutes.

sities of the dopant peak and the host zirconium peak in the XPS spectrum taken from the grain-boundary area, respectively. $P_{D(o)}$ and $P_{Zr(o)}$ are the integrated intensities of the dopant peak and the host zirconium peak in the XPS spectrum taken from the grain-bulk area, respectively. ξ_D and ξ_{Zr} are relative elemental sensitivity factors of the cerium ion (or the dopant ion) and the zirconium ion for XPS, respectively. The segregation factors of the cerium and dopants ions calculated using the equation 3 are listed in Table 1. Microstructures of the base Ce-TZP and doped Ce-TZPs were compared in Fig. 13.

IV. Discussion

1. The kinetics of normal isothermal grain growth

The driving force for the increase in the average grain size of a polycrystalline material is a chemical potential gradient caused by the pressure difference across the grain boundary which drives atoms across the boundary. From this concept the familiar square law of grain growth for pure single-phase materials was derived as following.

$$D^2-D_o^2=k_a t \quad (3)$$

where D, D_o, k_a and t is grown size of grain by heat treatment, initial grain-size, the grain-growth constant for pure polycrystalline material and time, respectively. The k_a can be expressed as following.[22]

$$k_a=4\alpha a^3 D_a \gamma/w\,k\,T \quad (4)$$

where α, a, D_a, γ, W, k, and T are a constant of the order of unity, the lattice parameter, diffusivity of atom moving across the boundary in pure polycrystalline material, grain boundary energy, grain boundary width, Boltzman constant, and temperature. Based on Cahn's theory,[27] Brook discussed an effect of impurity present in the form of solid solution on mobility of grain boundary.

$$M_i=M_a/(1+4\Phi WSC_o a^2) \quad (5)$$

where M_i and M_a are mobilities of grain boundary in impure and pure polycrystalline material, respectively. Also Φ, S, and C_o are volume concentraion of atoms, segregation factor, and the bulk impurity-concentration. For quantitative analysis it was assumed, in this study, that shape of grains was tetrakaidecahedron. Using Brook's concepts and this assumption the velocity of grain boundary in impure polycrystalline material, (dD/dt), can be expressed as the following.

$$v_i=dD/dt=16\alpha[M_a(S-1)a\gamma]/[4\Phi SC_T WD^2] \quad (6)$$

Equation 6 can be rewritten as the following equation in term of the grain growth constant, k_i, by integraion of Equation 6.

$$D^3-D_o^3=k_i t \quad (7)$$

From integration of Equation 6 and a comparison with Equation 7, the following equation can be obtained.

$$k_i=48\alpha[M_a(S-1)a\gamma]/[4\Phi SC_T W] \quad (8)$$

In the case of the Ce-TZP and Ce-TZP/Nb_2O_5, both the square law and cubic law of grain-growth gave adequate representation of the grain-growth kinetics of those materials annealed at 1550°C. However, since the segregation factor of the cerium ion (1.3) in the base Ce-TZP and Ce-TZP/Nb_2O_5 was too small, the condition for the cubic grain-growth, $1<<8(W/D)(S-1)$,[22,23,41] was not satisfied (with assumption of W=600Å, D=1.89 and 5.39 μm, respectively, thus, 8(W/D)(S-1)=0.076 and 0.027, respectively). Therefore, grain-growth kinetics in the base Ce-TZP and the Ce-TZP/Nb_2O_5 were analyzed using the square law of grain growth. However, in the case of Ce-TZP/MnO it was found that with the assumption of W=600Å and D=1.15 μm the value of f(W/D)(S-1) was much bigger than unity ($4\Phi WSC_0a^2=2640$). Thus, in the case of Ce-TZP/MnO the conditions for the cubic grain-growth were satisfied approximately. Thus, the grain-growth kinetics of Ce-TZP/MnO was analyzed with the cubic law of grain-growth.

2. Effect of defect structure caused by dopants on the kinetics of grain growth

The major defect in pure zirconia is an oxygen vacancy because the free energy of formation of anion vacancy is smaller than that of cation vacancy.[35] Since the diffusion of oxygen is very fast due to the preexistence of oxygen vacancy the mobility of grain boundary in the polycrystalline zirconia is determined by the zirconium vacancy. When some amounts of aliovalent dopants are added to the pure zirconia the concentration of the oxygen vacancy changes. This change in the concentration of the oxygen vacancy affects the creation of the zirconium vacancy. Thus, the grain-growth kinetics is affected by the addition of the dopant. It will be shown that the changes in defect structure and grain-growth kinetics for the base Ce-TZP and for the doped Ce-TZPs.

2-1. The base Ce-TZP

Pure CeO_2 has an intrinsic anion vacancies compensated by concurrent reduction of Ce^{+4} to Ce^{+3}. This intrinsic property is retained also in the base Ce-TZP with the absence of aliovalent dopants. The amount of Ce^{+3} ion in the base Ce-TZP is good enough to predominate the charge of grain boundary in the base Ce-TZP between 1000°C and 2000°C although small amount of Zr^{+4} ion is intrinsically reduced to Zr^{+3} ion.[36] The equation for predominant defects in the base Ce-TZP is written by

$$2Ce_{Zr}+O_o \xrightarrow{ZrO_2} (1/2)O_2+V_o^{\cdot\cdot}+2\,Ce_{Zr}' \tag{9}$$

where Ce_{Zr} and O_o are Ce^{+4} ion and O^{-2} ion occupying lattice site of Zr^{+4} ion and O^{-2} ion respectively, $V_o^{\cdot\cdot}$ is vacancy of oxygen, and Ce_{Zr}' is Ce^{+3} ion occupying lattice site of Zr^{+4} ion. Naik and Tien[36-37] found a correlation between electrical conductivity, σ, and oxygen deficiency, x, in CeO_{2-x} between 900 and 1329°C. Based on Naik and Tien's results Hwang and Chen[35] estimated the concentration of Ce^{+3} ion in the Ce-TZP for higher temperature range. From their estimation it is expected that the concentration of Ce^{+3} ion, $[Ce_{Zr}']$, in the base Ce-TZP at 1550°C would be 0.004. The equilibrium constant, K_1, for the reaction in Equation 9 can be written in the following equation:

$$K_1=(P_{O_2}^{1/2}[V_o^{\cdot\cdot}]\,[Ce_{Zr}']^2)/[Ce_{Zr}]^2 \tag{10}$$

Where partial pressure of oxygen, P_{O_2}, and concentration of Ce^{+4} ion, $[Ce_{Zr}]$, in the base Ce-TZP are 0.2 and 0.12, respectively. Electroneutrality condition for the reaction in Equation 9 gives the following equation:

$$2[V_o^{\cdot\cdot}]=[Ce_{Zr}'] \tag{11}$$

Thus, from the estimation of the concentration of Ce^{+3}, $[Ce_{Zr}']$, in Equation 11, $[V_o^{\cdot\cdot}]$ in the base Ce-TZP was found to be 0.002. The concentration of $[V_{Zr}'''']$, in turn, is dictated by the Schottky defect reaction:

$$\text{null} \rightarrow [V_{Zr}'''']+2[V_o^{\cdot\cdot}] \tag{12}$$

The equilibrium constant, K_s, for the Schottky reaction is given by the following equation:

$$K_s=[V_{Zr}'''']\,[V_o^{\cdot\cdot}]^2 \tag{13}$$

Based on Dwivedi and Cormack's[58] thermodynamical data on tetragonal zirconia was calculated to be 7.781×10^{-19} at 1550°C. Thus, $[V_{Zr}'''']$, in the base Ce-TZP is expressed in the following equation:

$$[V_{Zr}'''']=K_s/[V_o^{\cdot\cdot}]^2 \tag{14}$$

Using Hwang and Chen's estimation and Dwivedi and Cormack's data described before, the concentration of zirconium vacancy, $[V_{Zr}'''']$, was calculated to be 1.968×10^{-13}. Since the diffusion of oxygen is very fast due to the preexistence of oxygen vacancies the boundary motion in the base Ce-TZP is controlled by the slower diffusion of the cations of zirconium and cerium.[35] However, since relative amount of zirconium ion in the base Ce-TZP is much greater than that of cerium ion diffusion of the zirconium ion was considered as the rate-determining step of the grain growth. The vacancies of the zirconium ion with strong negative-effective-charge, created through the Schottky reaction, are attracted by the positively charged grain-boundary. The diffusion of the zirconium ion to the grain boundary is proceeded through strong attraction between these cationic vacancies with high negativity and positively charged grain-boundary. Thus, the flux of the zirconium ion to the grain boundary is generated by the diffusion of the cationic vacancies.

2-2. 1 mol % Nb_2O_5 doped Ce-TZP

Nb_2O_5, which was added as a pentavalent dopant to the base Ce-TZP, was expected to stay in the grain bulk in the base Ce-TZP due to repulsion between positively charged grain boundaries and Nb^{+5} ions with single positive effective charge. If the intrinsic property of Ce^{+4}/Ce^{+3} reduction can be extended to Ce-TZP/Nb_2O_5 the defect

structure caused by the addition of pentavalent dopant, Nb_2O_5, can be formulated. There are three defect structures in Ce-TZP/Nb_2O_5. First equation is

$$2Ce_{Zr}+Oo \xrightarrow{ZrO_2} (1/2)O_2+V_o^{\cdot\cdot}+2Ce_{Zr}' \quad (15)$$

The equilibrium kinetic constant, K_1, for the reaction in Equation 15 can be expressed by the same equation as Equation 10. If it is assumed that a positive charge of $Nb_{Zr}^{\cdot}$, caused by the addition of the niobium oxide, is compensated with a negative charge of Ce_{Zr}', created by reduction of Ce^{+4} ion to Ce^{+3} ion second equation of dissolution reaction of Nb_2O_5 into the base Ce-TZP can be written as

$$Nb_2O_5+2Ce_{Zr} \xrightarrow{ZrO_2} 2Ce_{Zr}'+2Nb_{Zr}^{\cdot}+4O_o+(1/2)O_2 \quad (16)$$

As assumed before, since Schottky reaction occurs in the Ce-TZP third equation is the same as Equation 9. The equilibrium constant, K_s, of Schottky reaction in Ce-TZP/Nb_2O_5 can be expressed by the same equation as Equation 13. Overall electroneutrality condition for the three defect reactions gives the following equation:

$$[Ce_{Zr}']=[Nb_{Zr}^{\cdot}]+2[V_o^{\cdot\cdot}] \quad (17)$$

Since from Hwang and Chen's estimation, $[Ce_{Zr}']$ is 0.022 and $[Nb_{Zr}^{\cdot}]$ is 0.02, $[V_o^{\cdot\cdot}]$ was found to be 0.001 from Equation 14. Using Equation 10 the concentration of the zirconium vacancy, $[V_{Zr}^{""}]$, in the Ce-TZP/Nb_2O_5 can be also found to be 7.871×10^{-15}. This increased concentration of the zirconium vacancy enhances diffusivity of the zirconium ion. This improvement of diffusivity of the zirconium ion increases the boundary mobility significantly. Thus, the enhancement of the concentration of the zirconium vacancy significantly increases the grain-growth constant, k_a, of Ce-TZP/Nb_2O_5, as compared to that of the base Ce-TZP. This fact can be proved through calculation of ratio of k_a for Ce-TZP/Nb_2O_5 and that for the base Ce-TZP. The ratio of for Ce-TZP/Nb_2O_5 and that for the base Ce-TZP can be written as

$$k_a(Nb)/k_a(Base)=4[a^3(Nb)/W(Nb)][D_a^{Zr}(Nb)/kT]\gamma(Nb)/4[a^3(Base)/W(Base)][D_a^{Zr}(Base)/kT]\gamma(Base) \quad (18)$$

where $k_a(Nb)$ and $k_a(Base)$ are grain-growth constants of Ce-TZP/Nb_2O_5 and the base Ce-TZP, respectively, $a^3(Nb)$ and $a^3(Base)$ are lattice parameters of Ce-TZP/Nb_2O_5 and the base Ce-TZP, respectively, W (Nb) and W (Base) are grain-boundary width of Ce-TZP/Nb_2O_5 and the base Ce-TZP, respectively, $D_a^{Zr}(Nb)$ and $D_a^{Zr}(Base)$ are diffusivity constants of zirconium ion in Ce-TZP/Nb_2O_5 and the base Ce-TZP, respectively. Due to the similar segregation behavior of solute in both materials grain-boundary width, W and grain boundary energy, γ, for both materials are assumed to be the same, Thus, Equation 18 can be rewritten as follows:

$$k_a(Nb)/k_a(Base)=a^3(Nb)D_a^{Zr}(Nb)/a^3(Base)D_a^{Zr}(Base) \quad (19)$$

If diffusion of the zirconium ions proceed with vacancy diffusion mechanism Equation 19 can be expressed by

$$k_a(Nb)/k_a(Base)=a^3(Nb)D_v^{Zr}(Nb)X_v^{Zr}(Nb)/a^3(Base)D_v^{Zr}(Base)X_v^{Zr}(Base) \quad (20)$$

where $D_v^{Zr}(Nb)$ and $D_v^{Zr}(Base)$ are diffusivities of the zirconium vacancies in Ce-TZP/Nb_2O_5 and the base Ce-TZP, respectively, and $X_v^{Zr}(Nb)$ and $X_v^{Zr}(Base)$ are concentrations of vacancy of the zirconium ion in Ce-TZP/Nb_2O_5 and the base Ce-TZP, respectively. Since $D_v^{Zr}(Nb)$ and $D_v^{Zr}(Base)$ are equal Equation 20 can be rewritten in the following equation:

$$k_a(Nb)/k_a(Base)=a^3(Nb))X_v^{Zr}(Nb)/a^3(Base)X_v^{Zr}(Base) \quad (21)$$

Jorgensen and Weatbrook[38] showed effect of aliovalent dopant on lattice parameter of matrix. The radius of niobium ion (0.32Å) is smaller than that of zirconium and cerium ions (0.84Å and 0.97Å, respectively).[39] Therefore, a substitution of zirconium and cerium ions with niobium ion caused by formation of solid solution of Ce-TZP/Nb_2O_5 reduces the lattice parameter of the base Ce-TZP. However, since amount of substitution of the zirconium and the cerium ions with niobium ion is just 1 mol% it is not expected that reduction of lattice parameter of matrix changes significantly. From a calculation based on our experimental data of k_a it was found that value of $k_a(Nb)/k_a(Base)$ was 5.351 while the theoretically calculated value of $X_v^{Zr}(Nb)/X_v^{Zr}(Base)$ based on schottky defect mechanism was 4. From a good match between the experimental value and the theoretical value of $k_a(Nb)/k_a(Base)$ it was verified that addition of Nb_2O_5 to the base Ce-TZP enhanced the grain growth in the base Ce-TZP significantly through the increment of the concentration of the zirconium vacancy.

2-3. 1 mol% MnO doped Ce-TZP

MnO which was added as divalent dopant to the base Ce-TZP was expected to segregate on the grain boundaries in the base Ce-TZP strongly because of Coulombic attraction between positively charged grain boundaries and Mn^{+2} ions with double negative charge. The formation of defect caused by addition of 1 mol% MnO can be expressed by the following defect equations. First, the intrinsic reduction of Ce^{+4} ion to Ce^{+3} ion gives the following equation:

$$2Ce_{Zr}+O_o \xrightarrow{ZrO_2} (1/2)O_2+V_o^{\cdot\cdot}+2Ce_{Zr}' \quad (22)$$

The equilibrium constant, K_1, is expressed by the same equation as Equation 10. It is assumed that since Mn^{+2} ion is very easy to be oxidized Mn^{+2} ion is oxidized to be Mn^{+3} ion in the base Ce-TZP the reaction of dissolution of MnO into the base Ce-TZP can be written as

$$MnO \xrightarrow{ZrO_2} Mn_{Zr}^{\cdot}+O_o+(1/2)V_o^{\cdot\cdot} \quad (23)$$

where $Mn_{Zr}^{\cdot}$ is Mn^{+3} ion occupying lattice site of Zr^{+4} ion.

Overall electroneutrality condition can be written as

$$[Mn_{Zr}^{'}]+[Ce_{Zr}^{'}]=2[V_o^{\cdot\cdot}] \quad (24)$$

where $[Mn_{Zr}^{'}]$ and $[Ce_{Zr}^{'}]$ are 0.01 and 0.0002, respectively. From Equation 24 the concentration of the oxygen vacancy was found to be 0.005. If Schottky equilibrium is also maintained in Ce-TZP/MnO from Equation 24 and 13 the concentration of the zirconium vacancy was found to be 2.087×10^{-14}. Thus the concentration of the zirconium vacancy in Ce-TZP/MnO is found to be smaller than that in the base Ce-TZP. Thus, the reduction of the concentration of the zirconium vacancy suppresses the grain growth in the Ce-TZP. This can be rationalized from calculation of ratio of k_a for the Ce-TZP and k_i for Ce-TZP/MnO. The ratio of k_a for the base Ce-TZP and k_i for Ce-TZP/MnO can be written as

$$k_i(Mn)/k_a(Base)=[12\alpha M_a(Mn)(S-1)a(Mn)\gamma(Mn)/\Phi SC_T W(Mn)]/[4\alpha a^3(Base)M_a(Base)\gamma(Base)/W(Base)] \quad (25)$$

Where $M_a(Mn)$ and $M_a(Base)$ are mobilities of grain boundary in Ce-TZP/MnO and the base Ce-TZP, respectively, a (Mn) and a (Base) are lattice parameters of Ce-TZP/MnO and the base Ce-TZP, and $\gamma(Mn)$ and $\gamma(Base)$ are grain-boundary energies of Ce-TZP/MnO and the base Ce-TZP, respectively. It is expected that lattice parameter, grain-boundary energy, and grain-boundary width do not change much for both materials. Thus, Equation 25 can be reduced in the following equation:

$$k_i(Mn)/k_a(Base)=3D_a^{Zr}(Mn)(S-1)/\Phi a^3(Base)D_a^{Zr}(Base)SC_T \quad (26)$$

As assumed before, If diffusion of the zirconium ions proceeds with vacancy diffusion mechanism Equation 26 can be written as

$$k_i(Mn)/k_a(Base)=3X_v^{Zr}(Mn)(S-1)/\Phi a^2(Base)X_v^{Zr}(Base)SC_T \quad (27)$$

3. Effect of solute segregation caused by the aliovalent dopants on the kinetics of grain growth

It was found that solutes decrease the free energy of the system by lowering interfacial energy caused by being adsorbed at the interface and that the degree by which the interfacial energy is lowered is directly related to the amount of solute segregation on grain boundary.[25,26,40] Under these circumstances the concentration of solute in the grain boundary, C_B, is higher than that in the grain bulk, C_o. approximately for low concentrations of solute in the matrix the equilibrium grain-boundary enrichment ratio, (C_B/C_o), is given by

$$C_B/C_o \sim \exp(Q/RT) \quad (28)$$

The magnitude of the grain-boundary drag caused by solute segregation on the boundary depends on the adsorption energy of solutes on grain boundary and the concentration of solute in the grain boundary. As we discribed before for ceramic oxide materials there is normally a boundary charge compenstaed by space-charge cloud of the opposite sign adjacent to the grain boundary in which the concentrations of lattice defects and dopants with effective charge are different from the concentrations of those far from a boundary. The primary factor leading to the equilibrium solute segregation on grain boundary is probably the electrostatic potential near grain boundary.[25,26,35] when the aliovalent dopant alters the concentrations of lattice defects in the crystal the magnitude and sign of the boundary charge and space charge change. That is the electrostatic potential changes upon the addition of aliovalent dopant. This change of the electrostatic potential induces change of the segregation behavior of solute on grain boundary. The second factor leading to grain-boundary segregation is the reduction in strain energy of solutes at and near the boundary. At the core of the boundary there is some fraction of already distorted sites for which the strain caused by solute addition is smaller than lattice. The preference for filling these distorted sites depends on the difference in energies for the solutes at the distorted sites and in the lattice.[40] For ceramic oxide materials the primary factor of electrostatic potential is more important than the second factor of strain energy in the behavior of the solute segregation. Thus, our discussion will be focused on the space-charge concept.

4. Effect of solute segregation on the kinetics of the grain growth in the base Ce-TZP and Ce-TZP/MnO

It was observed that Mn^{+2} segregated on the grain boundaries in Ce-TZP strongly with the segregation factor of 6.4 and that experimental measurements of grain grwoth in the Ce-TZP/MnO agreed the cubic law of grain growth. These facts means that the grain growth of Ce-TZP/MnO, not the base Ce-TZP and Ce-TZP/Nb_2O_5, is controlled by impurity drag in accord with the model originally developed by Cahn and advanced by Brook. As we described before, the grain-growth constant, k_i, for the cubic law is affected by various factors. For qualitative analysis of the kinetics of the grain growth in Ce-TZP/MnO each term in Equation 8 was considered. Φ term and C_T term in Equation 5 stay at the same level as those of the base Ce-TZP because total amount of solute is equal in both materials. It is expected that w term in Equation 5 are enhanced, not much as compared to the base Ce-TZP, due to the strong segregation of the manganese ions on grain boundaries. Since the amount of MnO added to the base Ce-TZP is very small (1 mol%) the strong segregation of the manganese ions on grain boundaries does not increase the width of grain boundary much. It is also expected that lattice parameter, a, of the base Ce-TZP does not change because almost all of manganese ions segregate on grain boundary and the amount of the manganese ions added to the base Ce-TZP is very small. γ is assumed to be almost same as that of the base Ce-TZP although γ is expected to vary by more than a factor of 2 to 3.[35] Thus, the grain-growth constant,

k_i, for Ce-TZP/MnO is affected by the segregation of solute on grain boundary and the mobility mainly. Since the k_i is inversely proportional to the degree of solute segregation, as described in Equation 5, one reason of suppression of grain growth in Ce-TZP/MnO, as compared to that of the base Ce-TZP, can be the strong segregation of the manganese ions on grain boundaries in the base Ce-TZP. the other is the mobility of grain boundary. Since as shown by Nernst-Einstein equation the mobility is proportional to the diffusivity the grain growth constant, is proportional to the diffusivity. As described before, since the zirconium ion is the slowest diffusing specis in the base Ce-TZP the mobility of grain boundary is affected by the amount of zirconium vacancy existing in the Ce-TZP. As shown before, reduction of the concentration of the zirconium ion in the Ce-TZP/MnO, as compared to that of the base Ce-TZP, caused reduction of the mobility of grain boundary. Thus, the reduction of the concentration of the zirconium vacancy, caused by the addition of MnO to the base Ce-TZP, induces the suppression of grain growth in the base Ce-TZP.

V. Conclusions

1. The grain growth in the base Ce-TZP and Ce-TZP/Nb_2O_5 shows adequate match with the square law of grain growth.

2. The grain growth in the Ce-TZP/MnO obeys the cubic law of grain growth.

3. The trivalent cation of Ce^{+3}, created by the intrinsic property of reduction of CeO_2, segregates weakly on grain boundary in the base Ce-TZP and Ce-TZP/Nb_2O_5 with segregation factor of 1.3 for both materials

4. The divalent cation, Mn^{+2}, segregates strongly on grain boundary in the Ce-TZP/MnO with the segregation factor of 6.4.

5. The pentavalent cation, Nb^{+5}, does not segregate on grain boundary in Ce-TZP/Nb_2O_5 due to repulsion between Nb^{+5} ion with positive effective charge and positively charged grain boundary.

References

1. R. Stevens, "Zirconia and Zirconia Ceramics," 1-2, 18-20, Magnesium Elektron Ltd., 1986.
2. E. C. Subbarao, "Zirconia-An Overview," 1-24 in Advances in Ceramics, Vol. 3, Science and Technology of Zirconia I. Edited by A. H. Heuer and L. W. Hobbs, American Ceramic Society, Columbus, Ohio, 1986.
3. E. C. Subbarao, H. S. Maiti and K. K. Srivastava, "Martensitic Transformation in Zirconia," *Phys. Status Solid*, A, **21**, 9-40 (1974).
4. V. S. Stubican and J. R. Hellmann, "Phase Equilibria in Some Zirconia Systems," 25-37 in Advances in Ceramics, Vol. 3 Science and Technology of Zirconia I. Edited by A. H. Heuer and L. W. Hobbs, American Ceramic Society, Columbia, Ohio, 1981.
5. D. L. Porter and A. H. Heuer, "Microstructural Development in MgO-Partially Stabilized Zirconia (Mg-PSZ)," *J. Am. Ceram. Soc.*, **62**(5-6), 298-305 (1979).
6. R. H. J. Hannink, "Growth Morphology of the Tetragonal Phase Partially Stabilized Zirconia (Mg-PSZ)," *J. Mater. Sci.*, **13**, 2487-2496 (1978).
7. R. C. Garvie and P. S. Nicholson, "Structure and Thermomechanical Properties of Partially Stabilized Zirconia in CaO-ZrO_2 System," *J. Am. Ceram. Soc.*, **55**(3), 152-157 (1972).
8. M. Yoshimura, "Phase Stability of Zirconia," *Am. Ceram. Soc. bull.*, **67**(12), 1950-1955 (1988).
9. K. Tsukuma, "Mechanical Properties and Thermal Stability of CeO_2 Containing Tetragonal Zirconia Polycrystals," *Am. Ceram. Soc. Bull.*, **65**(10), 1386-1389 (1986).
10. K. Tsukuma and M. Shimada, "Strength, Fracture Toughness and Vickers Hardness of CeO_2-Stabilized Tetragonal ZrO_2 Polycrystals (Ce-TZP)," *J. Mater. Sci.*, **20**, 1178-1184 (1985).
11. E. Tani, M. Yoshinura and S. Somiya, "Revised Phase Diagram of the System-Below 1400°C," *J. am. Ceram. Soc.*, **66**(7). 506-510 (1983).
12. P. Duwez and G. Odell, "Phase Relationships in the System Zirconia-Ceria," *J. Am. Ceram. Soc.*, **33**(9), 274-283 (1950).
13. M. G. Scott, "Phase Relationships in the Zirconia Yttria System," *J. Mater. Sci.*, **10**, 1527-1535 (1975).
14. A. G. Evans, N. Burlingame, M. Drory and W. M. Kriven, "Martensitic Transformations in Zirconia-Particle Size Effects and Toughening," *Acta Metall.*, **29**(2), 447-456 (1986).
15 F. F. Lange and D J. Green, "Effect of Inclusion Size on the Retention of Tetragonal ZrO_2: Theory and Experiments," 217-225 in Advances in Ceramics, Vol. 3, Science and Technology of Zirconia Edited by A. H. Heuer and L. W. Hobbs. American Ceramic Society, Columbus, Ohio, 1981.
16. K. Gupta, F. F. Lange and J. H. Bechtold, "Effect of Stress-Induced Phase Transformation on the Properties of Polycrystalline Zirconia Containing Metastable Tetragonal Phase," *J. Mater. Sci.*, **13**, 1178-1184 (1978).
17. A. H. Heuer, N. Claussen, W. M. Kriven and M. Ruhle, "Stability of Tetragonal ZrO_2 Particles in Ceramic Matrices," *J. Am. Ceram. Soc.*, **65**(12), 642-650 (1982).
18. R. H. J. Hannink, K. A. Johnson, R. T. Pascoe and R. C. Garvie, "Microstructural Changes During Isothermal Aging of a Calcia Partially-Stabilized Zirconia Alloy," *Adv. Ceram.*, **3**, 116-136 (1981).
19. P. F. Becher, M. V. Swain and M. K. Ferver, "Relation of Transformation Temperature to the Fracture Toughness of Transformation-Toughened Ceramics," *J. Mater Sci.*, **22**, 76-84 (1987).
20. K. Tsukuma and M. Shimada, "Strength, Fracture Toughness of CeO_2-Stabilized Tetragonal ZrO_2 Polycrystals (Ce-TZP)," *J. Mater. Sci.*, **20**, 1178-1184 (1985).
21. H. Tsubakino and R. Nozato, "Effect of Alumina Addition on the Tetragonal-to-Monoclinic Phase Transformation in Zirconia-3 mol % Yittria," *J. Am. Ceram. Soc.*, **74**(2), 440-443 (1991).
22. R. J. Brook, "Controlled Grain Growth," 331-363 in Trea-

tise on Materials Science and Technology, Vol. 9, Edited by F. F. Y. Wang, Academic Press, New York, 1976.
23. P. J. Jorgensen, "Final Stage Sintering and Grain Growth in Oxides," Defects and Transport in Oxides, Battelle Colloquium, Columbus, Ohio, 1973.
24. P. E. C. Franken and A. P. Gehring, "Grain Boundary Analysis of MgO-Doped Al_2O_3," *J. Mater. Sci.*, **16**, 384-388 (1981).
25. W. D. Kingery, "Plausible Concepts Necessary and Sufficient for Intertretation of Ceramic Grain-Boundary Phenomena: I, Grain-Boundary Characteristics, Structure, and Electrostatic Potential," *J. Am. Ceram. Soc.*, **57**(1), 1-8 (1974).
26. W. D. Kingery, "Plausible Concepts Necessary and Sufficient for Interpretation of Ceramic Grain-Boundary Phenomena: II, Solute Segregation, Grain-Boundary Diffusion and Grneral Discussion," *J. Am. Ceram. Soc.*, **57**(2), 74-83 (1974).
27. J. W. Cahn, "The Impurity-Drag Effect in Grain Boundary Motion," *Acta Metall.*, **10**, 789-798 (1962).
28. D. J. Srolobvitz, R. Eykholt, D. M. Barnett and J. P. Hirth, "Moving Discommensurations Interacting with Diffusing Impurities," *Physical Review B*, **35**(12), 6107-6121 (1987).
29. K. Lucke and H. P. Stuwe, "On the Theory of Impurity Controlled Grain Boundary Motion," *Acta Metall.*, **19**, 1087-1099 (1971).
30. M. Hillert, "On the Theory of Normal and Abnormal Grain Growth," *Acta Metall.*, **13**, 227-238 (1965).
31. M. F. Yan and D. W. Joghnson J. R., "Impurity-Induced Exaggerated Grain Growth in Mn-Zn Ferrites," *J. Am. Ceram. Soc.*, **61**(7-8), 342-349 (1978).
32. J. Danials and K. H. Hardyl, "Defect Chemistry and Electrical Conductivity of Barium Doped Titanate Ceramics," *Philips Research Reports.*, **31**(6), 489-504 (1976).
33. C. J. Peng and Y. M. Chiang, "Grain Growth in Doner-Doped $SrTiO_3$," *J. Mater. Res.*, **5**(6), 1237-1245 (1990).
34. C. D. Wagner, "Handbook of X-ray Photoelectron Spectroscopy" Perkin-Elmer Corporation, Minnesota, (1979).
35. S. L. Hwang and I. W. Chen, "Grain Size Control of Tetragonal Zirconia Polycrystals Using the Space Charge Concept," *J. Am. Ceram. Soc.*, **73**(11), 3269-3277 (1990).
36. I. K. Naik and T. Y. Tien, "Small Polaron Mobility in Non-Stroichiometric Cerium Dioxides," *J. Phys. chem. Solids*, **38**(3), 311-315 (1978).
37. I. K. Naik and T. Y. Tien, "Electrical Conduction in Nb_2O_5-doped Cerium Oxides," *J. Electrochem. Soc.*, **126**(4), 562-566 (1979).
38. P. J. Jorgensen, "Final Stage Sintering and Grain Growth in Oxides," Defects and Transport in Oxides, Battelle Colloquium, Columbus, Ohio, 1973.
39. R. D. Shannon and C. T. Prewitt, Effective Optimum Radii in Oxides and Fluorides," *Acta Cryst.*, **B25**, 925-945 (1969).
40. D. McLean, "Grain Boundaries in Metals." 36, Clarendon Press, Oxford, 1957.
41. R. J. Brook, "The Impurity-Drag Effect and Grain Growth Kinetics," *Scripta Metallurgica*, **2**(7), 375-378 (1968).